Tracing the Status of Silica Fume in Cementitious Materials with Raman Microscope

Yanfei Yue[ab], Jing Jing Wang[c**] and Yun Bai[b*]

[a] College of Materials Science and Engineering, Chongqing University, 174 Shazheng Street, Shapingba, Chongqing, China 400044

[b]Department of Civil, Environmental and Geomatic Engineering, University College London, Gower Street, London, UK, WC1E 6BT

[c]CRANN and AMBER Research Centres, Trinity College Dublin, Dublin 2, Dublin, Ireland

Abstract

Silica fume (SF) is an essential material for formulating high performance concrete (HPC). However, its small particle size could cause safety-hazards. Although replacing SF powder with slurry can somehow avoid the potential bio-toxicity, its long-term stability within cementitious materials is unknown. In this study, Raman microscope which combines Raman spectroscopy with light-optical microscope was successfully applied to characterise the composition and morphology of SF in original slurry and hydrated SF-Portland cement (PC) pastes. The unhydrated SF-agglomerates were clearly detected in the original SF slurry and the 22-hour and 6-month hydrated SF-PC pastes.

Keywords: Amorphous silica; Cementitious materials; Raman microscope; Raman spectroscopy; Silica fume.

1. INTRODUCTION

Silica fume (SF) is a super-fine material consisting mainly of amorphous silica spheres (85% - 95%) with an average particle diameter of 150nm[1, 2]. It is a supplementary cementitious material (SCM) widely used in construction industry for manufacturing high performance concrete (HPC) with promising properties such as supreme long-term durability and high strength[2-4]. These positive actions of SF can be mainly attributed to the following two mechanisms: (i) *excellent pozzolanic reactivity*. As SF mainly consists of highly reactive amorphous silica, it can react with calcium hydroxide (CH) (usually arising from the hydration of Portland cement) to form calcium silicate hydrate (CSH) - the most important binding and

* Dr Yun Bai. Email: yun.bai@ucl.ac.uk. Tel: +44(0)20 76792386.

** Dr Jing Jing Wang. Email: JJWANG@tcd.ie. Tel: 00353 18964633.

strength giving hydration product in cementitious materials; (ii) *physical filling effect*. Because of its very small particle size, SF can fill in the various pores in the hardened cement matrix and hence enhance the density and the strength of the hardened paste[5, 6]. Both mechanisms can lead to improved durability and strength. However, whilst SF has numerous advantages, it also has the common failing of nano-scale materials, i.e. potential safety hazards to living systems[7]. This is induced by the ultrafine particles of SF and thus could be easily absorbed through the skin, lungs or digestive tract, causing health risks to the living systems[8, 9]. Therefore, nowadays it is preferred to use SF slurry (i.e. SF in aqueous dispersions) with a typical solid content of 50 wt. %in practical operations. Although this can somehow avoid the safety hazards incurred to the operators to a certain extent and decrease the difficulty encountered from handling dry bulk powders, the potential safety hazards of the SF used in the slurry form still exist as the long-term stability and activity of unhydrated/hydrated SF in concretes is largely unknown.

In more detail, the following two aspects need to be clearly understood before SF slurry can be confidently used in civil engineering applications:

(i) *The status of SF particles in original SF slurry.* It is now well established that dry densified SF exists almost in the form of SF agglomerates, i.e. nano-spheres linked together into chains or clusters, rather than isolated spheres[10-12]. However, there is rare knowledge about the status of SF particles in the slurried SF and, if there are any SF agglomerates in the SF slurry, their status is also largely unknown. Hence, it is of great importance to identify the status of the SF particles in the SF slurry. Furthermore, as the breakdown of the agglomerates during mixing processes is highly relevant to the effectiveness of the crushing and shearing actions applied by the mixer, the information obtained could also be invaluable for guiding the *on-site* mixing operations.

(ii) *The status of SF within cementitious materials over different hydration time.* Theoretically speaking, the amorphous silica in the SF is considered to react with calcium hydroxide (CH) and thus transform into calcium silicate hydrate (CSH), making contribution to the strength improvement of the cement materials. However, unhydrated SF agglomerates were observed in the long-term hydrated cementitious materials fabricated by the dry densified SF, which could be attributed to the fact that the SF agglomerates may break down only partially in normal concrete mixing processes[10, 11]. The status and the stability of these unreacted agglomerates would cause another potential concern to the safety of the living systems exposed directly or indirectly to the concrete structures.

Currently, many techniques are employed to identify the morphology and the composition of SF and SF-containing cement products, such as Scanning Electron Microscopy (SEM) and Energy Dispersive X-Ray Spectroscopy (EDX)[10, 11]. SEM can provide clear figures of the morphology of SF agglomerates in the original dry densified powder and also the SF-containing hydrated cement pastes. However, it cannot illustrate the chemical composition of the SF and hence another quantitatively analysis facility needs to be applied simultaneously. At the same time, liquid sample cannot be analysed with high precision under the SEM. Whilst EDX could indicate the composition of SF, it can only give information on the elemental composition of SF such as Si and O, but not the chemical composition with intrinsic atomic-ratio (i.e. SiO_2). Raman spectroscopy, a vibrational spectroscopy, can provide 'fingerprint' information of molecular structures for solids, liquids and gases. It works on inelastic scattering that the Raman scattered light occurs at wavelength (frequency) being shifted up or down from the incident laser light. As this wavelength shift is specific to the chemical bonds and the symmetry of molecules, Raman scattered signal can thus be used to identify substances[13, 14]. Over routine characterisation tools, Raman spectroscopy showcases unique advantages in characterising chemical composition not only for crystalline but also amorphous phases – which explores a much wide analysing area in cement and concrete such as the identification of amorphous silica (SiO_2) in SF. Furthermore, the application of Raman microscope which combines Raman spectroscopy with light-optical microscopy offers a promising analysis tool for identifying both the chemical composition and physical morphology of the SF-containing cementitious materials.

In the current study, attempts were made to establish a protocol of using Raman spectroscopy to firstly identify the status of SF in the original SF slurry and then to trace the status of SF within cementitious materials at the nano-scale over different time scales, namely early (about 22h) and long-term (six months) hydration periods. Light-optical microscope was simultaneously used to characterise the morphology of various samples.

2. EXPERIMENTAL

2.1 SF slurry and diluted SF slurry

The as-received SF slurry, a dark-grey slurry with water content of 50%, was used as the raw material in this study. Its chemical composition is given in Table 1. To characterise the individual SF particles with Raman spectroscopy, diluted SF slurry was also prepared at a

slurry-to-water ratio of 1:5 by hand mixing in order to achieve a better dispersion of the SF particles before the Raman characterisation.

2.2 SF blended paste

The Portland cement (PC) used in this study was CEM I (in accordance with BS EN 197-1:2011 [15]) and its chemical composition is also shown in Table 1. The SF-bearing PC paste was prepared by replacing 8% of PC with SF (solid SF content in the SF slurry) (a typical level of SF used in practice) at a water/binder of 0.40, in order to obtain a workable mix in terms of the mini-slump value in the range of 55±5 mm. Immediately after mixing, the paste was poured into a small cell which was then covered with a glass slide to avoid the loss of moisture. After 22 hours, a small part of the paste samples was analysed under Raman microscope, and the remaining samples were removed from the cell and wrapped with a water saturated hessian, which were then sealed in a plastic sample bag and stored in a curing room at a constant temperature of 20±1^{o}C for around 6 months. The wet hessian was regularly checked and replaced once the moisture level was low.

Table 1 Chemical composition of Portland cement and silica fume

Oxides/%	SiO_2	Al_2O_3	Fe_2O_3	CaO	MgO	K_2O	Na_2O	SO_3
SF	93.00	0.70	1.20	0.30	1.20	1.80	1.50	0.30
PC	23.00	6.15	2.95	61.30	1.80	0.68	0.22	2.50

2.3 Raman microscope – Raman spectrometer combined with light-optical microscope

Raman spectroscopy was applied for qualitative identification of the phases existing both in the SF and in the hardened cement pastes, whereas optical microscope was employed to characterise the dispersion of the silica nano-particles and the morphology of various hydrated phases. Raman spectra were recorded at a controlled temperature of 20℃ via a micro-Raman spectroscopy equipped with a Charged Coupled Device (CCD) detector. The 488nm (Ar+) laser was used as excitation source. The laser beam was focused onto the samples through an appropriate microscope objective (as detailed below). The measured power at the sampling level was controlled at about 0.7mW. This low power level was purposely selected to avoid the overheating incurred from the dark-grey SF samples under the laser interrogation. The Raman spectra were recorded with exposure time of 10s and accumulations of 10 in order to improve the signal-to-noise ratio (SNR). Optical photograph

was recorded with the objectives at different magnifications (10x, 50x and 100x) in order to acquire the appropriate resolution and feature of the images.

3. RESULTS AND DISCUSSION

3.1 Characterisation of SF slurry with Raman microscope

3.1.1 Original SF slurry

In this study, a light-optical micrograph of original SF slurry was first recorded under 100x magnification. As shown in Fig. 1(a), the obtained micrograph was dominated by a grey 'background' with some randomly distributed white shining fragments and some relatively big substances in grey-dark colour. In order to characterise the chemical composition of the SF using Raman Spectroscopy with sufficient accuracy, two white coloured substances were selected (the background will be discussed later) for Raman analysis, i.e. point A and B in Fig. 1(a). Based on the preliminary trials, the laser with the wavelength of 488nm showed superior excitation and also negligible thermal damage, which was, hence, applied here. The recorded Raman spectra of these two test points are presented in Fig.1(b).

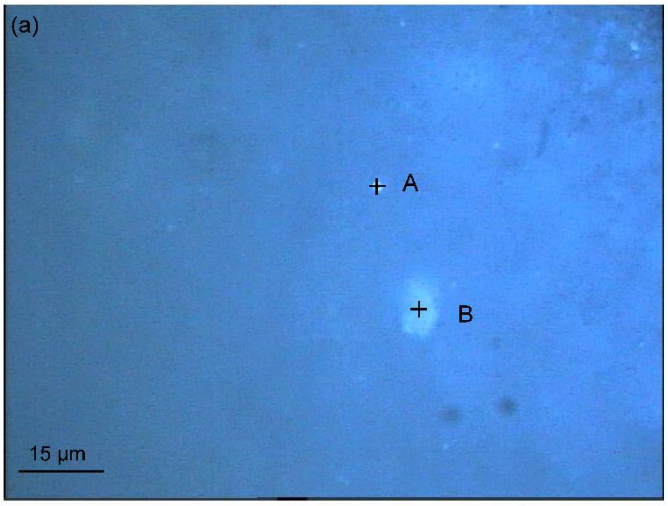

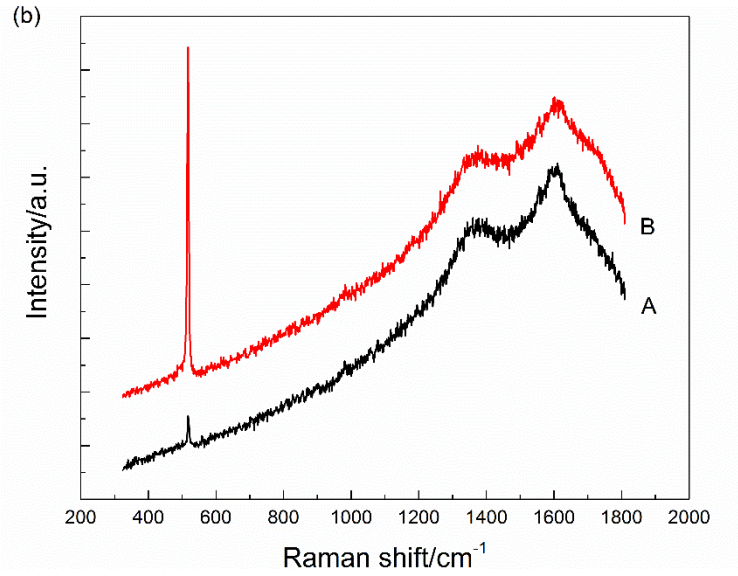

Fig. 1.(a) Light-optical micrograph of original SF slurry (100x). (b) Raman spectra of sampling points A and B as shown in (a).

As can be seen from Fig. 1, point A was a white shining spot containing some amorphous silica as indicated by the broad feature extending from about 350 cm^{-1} to 540 cm^{-1} in related Raman spectrum in Fig. 1(b)[16, 17].In addition, the weak Raman peak emerged at around 518 cm^{-1} could be attributed to the residual silicon crystals existing in the silica fume[18]. Please note that compared to the perfect-crystalline bulk silicon which normally emerges at 520 cm^{-1}, the Raman peak of crystallised silicon phase existed in raw SF shifted to a lower Raman frequency (518 cm^{-1}). From the literature, the decrease of particle size of the crystalline silicon components could cause red-shift of relevant Raman wavenumber, such as the polycrystalline silicon [18, 19].Point B was located at a white fragment of relatively large size, i.e. around 4 μm. Based on its sharp and intensive Raman peak at 518 cm^{-1} in Fig.1(b), it can be concluded that there is a considerable amount of silicon crystals in this fragment. At the same time, silica in both crystalline and amorphous states have been identified in Point B, as indicated by the weak shoulder at 486 cm^{-1} and the hump ranging between 350 and 540 cm^{-1} respectively[20, 21].The crystalline SiO_2 could come from the remaining unreacted quartz dust during the industrial production process and was possibly collected along with the SF by the bag-house. For both points A and B, there were strong carbon backgrounds with two pronounced bands at about 1359 cm^{-1} (D band) and 1609 cm^{-1} (G band) respectively, which could be attributed to the unreacted carbon in the SF[22].

3.1.2 Diluted SF slurry

It is generally accepted that most of the powdered SF exists in the form of silica agglomerates, rather than isolated spheres. However, there is very limited research about the morphology of the silica fume in slurry. As mentioned before, the original SF slurry used in the current study is a grey-black suspension with a solid/water ratio of 50:50. The preliminary Raman spectroscopy characterisation of this original SF slurry as shown in Fig.1(a) under the magnification of 100x indicated several white-shining points in the grey background of the suspension. The white fragments have been analysed under Raman spectroscopy in 3.1.1 and hence the discussion here will be focus on the grey background. To clearly identify the grey-dark background and any possible agglomeration of SF particles as well as to reveal the morphology of individual SF particles, the SF slurry was diluted at a water-to-SF slurry ratio of 5:1 which was then characterised under two optical objectives with different magnifications (i.e. 10x and 50x) together with the Raman spectroscopy analysis. The related results are shown in Fig. 2 below.

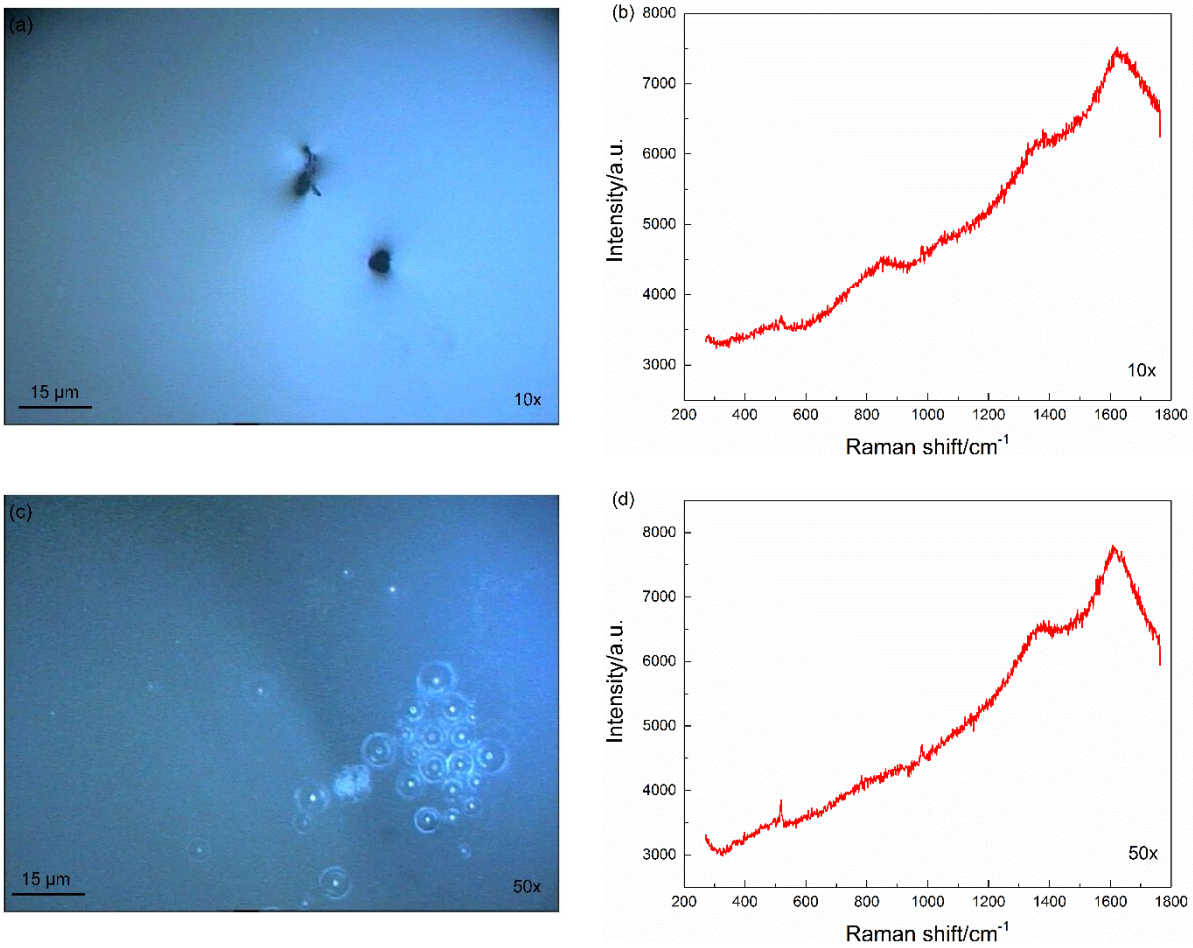

Fig. 2.(a) Light-optical micrograph of diluted SF slurry under 10x magnification. (b) Raman spectrum of diluted SF slurry under10x magnification. (c) Light-optical micrograph of diluted SF slurry under 50x magnification. (d) Raman spectrum of diluted SF slurry under 50x magnification.

As shown in Fig. 2(a), under the magnification of 10, various dark clusters (which could be the silica agglomerates) can be observed floating in the diluted slurry. Under the magnification of 50 (Fig. 2(c)), the silica agglomerates can be clearly observed, consisting of white/transparent spheres of individual SF particles. Under each magnification, Raman analysis was also carried out to identify the composition of the SF particles. As can be seen from Fig. 2(b) and Fig. 2(d), SF comprised of amorphous silica (the hump ranging from 350 to 540 cm^{-1}), silicon crystals (peak at 519 cm^{-1}), amorphous carbon (broad features centering at 1360 and 1609 cm^{-1}) and also uncertain impurities (peak at 981 cm^{-1}). However, sloping backgrounds can also be observed in Figs. 2(b) & 2(d) which impose strong disturbance to the Raman spectra – especially to the fingerprint band of amorphous silica, i.e. the hump between 350 and 540 cm^{-1}. This sloping background is probably induced by the fluorescence due to the re-emission of light by a substance when it relaxes to its ground state after being excited to a higher quantum state by incident energy[23]. To clearly identify this hump, background subtraction via a professional software was applied to correct the baseline of Fig. 2(d) – as its light-optical micrograph (i.e., Fig. 2(c)) shows clear evidence of the existence of amorphous silica particles/agglomerates. The Raman spectra after subtracting the background are presented in Fig. 3 below. As can be seen from Fig. 3(a), after subtracting the background, various Raman fingerprint bands become more evident than those in the original spectrum [Fig. 2(d)] – especially the hump showing the amorphous silica at 350-540 cm^{-1} which is further demonstrated in Fig. 3(b) as an inset in the wavenumber range 300-600 cm^{-1}.

The above results from the diluted SF slurry suggest that a considerable amount of silica agglomerates indeed exist in SF slurry. This would raise the concern over the possible existence of these agglomerates in the hardened SF-PC pastes due to the difficulty in dispersing the silica particles in concentrated matrix, because depending on the status of these unreacted SF particles, they could potentially cause safety issues to the living systems it exposed to – a typical issue facing the application of nano materials in real world [7-9].Therefore, some pilot studies were carried out in the current study to investigate the above issue and the related results are presented and discussed in the following section.

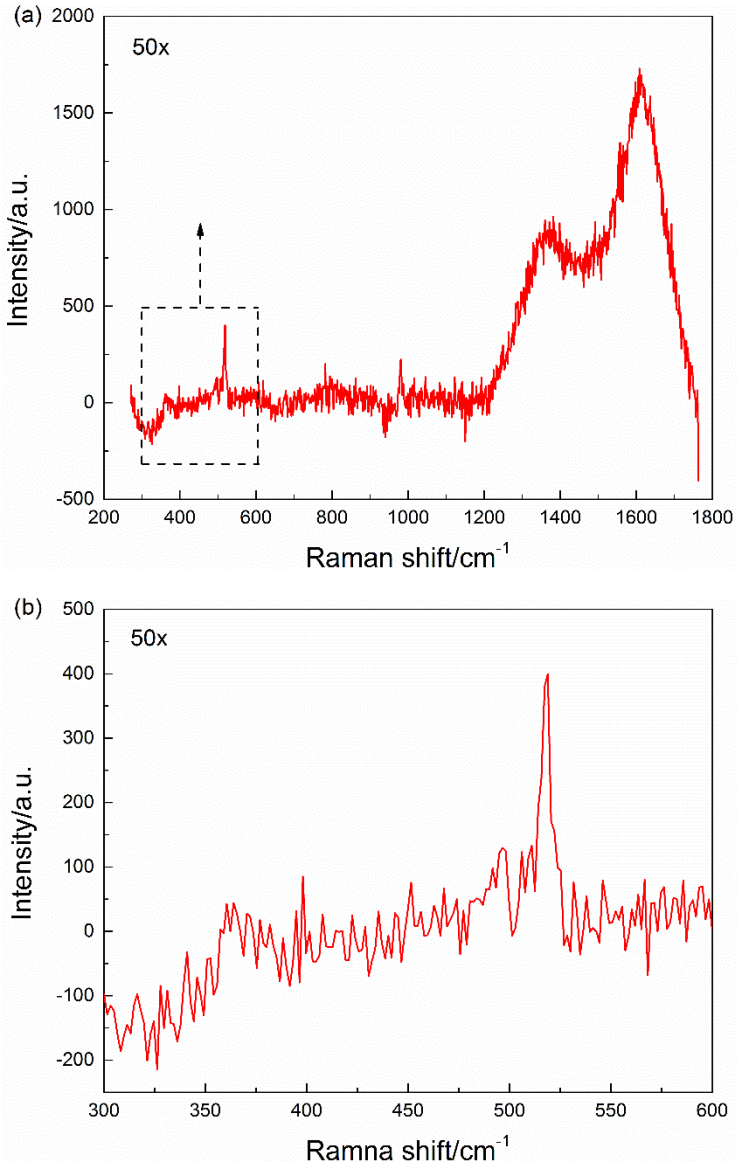

Fig. 3. (a) Raman spectrum of diluted SF slurry under 50x magnification after subtracting background. (b) Inset of Raman spectrum in the range of 300-600 cm^{-1}.

3.2 Tracing the status of SF in early and long-term hydrated SF-PC blended pastes with Raman microscope

3.2.1 SF-PC blended paste after 22 hours' hydration

To compare the effect of ongoing hydration on the status of SF in PC paste, the Raman analysis was firstly carried out on the SF blended paste after 22-hour hydration. This could identify the status of SF in early-age cementitious paste, which was then used to compare with the status of SF in PC paste observed after 6-month hydration in Section 3.2.2 below. It

was anticipated that a comparison between the status of SF in early-age and long-term SF-PC blended pastes would enable the identification of the effect of ongoing hydration on the status of SF agglomerates

As shown in Fig. 4, the paste in the selected area comprised of various white–transparent clusters, grey opaque areas and brown substances. Locations with typical features were then selected for Raman analysis and the related Raman spectra are shown in Fig. 5. The Raman analysis results from points A, B, D and E showed very similar Raman features and all of them were dominated by the carbonate peaks at 1085cm^{-1}(symmetric stretching of CO_3^{2-}) and 275 cm^{-1}(lattice vibration)[24, 25], along with humps of CSH phases in the range of 600-800 cm^{-1} and 950-1050 cm^{-1}[26, 27]. The carbonates are possibly formed from the carbonation during the 22-hour storage of the paste. Additionally, there was a peak in point D located at 857 cm^{-1}, which could be assigned to the unhydrated calcium silicate minerals[28, 29]. At the same time, it can be observed that a massive amount of CSH was generated at points F and C, as indicated by the strong humps at 600-800 cm^{-1}. Except for the abovementioned information, the results from points H and G could also provide invaluable information to assess the status of SF in the hydrated SF paste, which are discussed in the following paragraph.

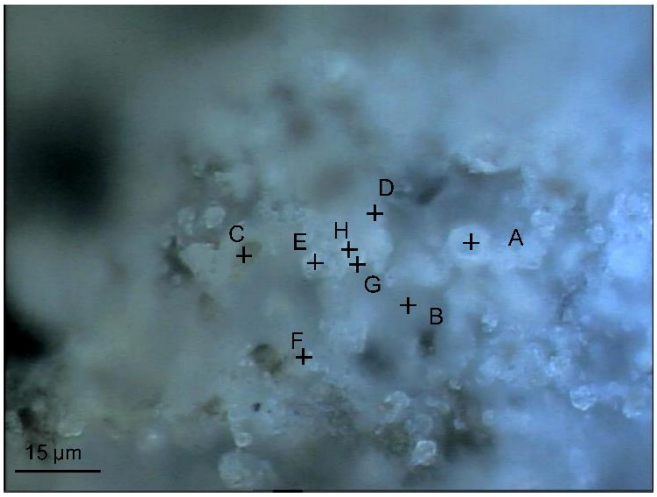

Fig. 4. Light-optical micrograph of the SF-PC blended paste after 22-hour hydration (100X)

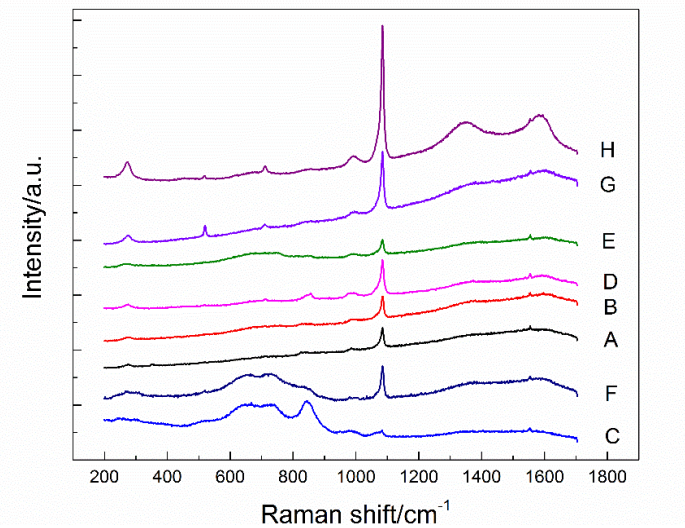

Fig. 5. Raman spectra of sampling points A-H as shown in Fig. 4

In point G, silicon crystal was identified, as manifested by the sharp peak at 519 cm^{-1}.In addition, various products were also recognised at this point, such as the carbonates (1085 cm^{-1},711 cm^{-1} and 275 cm^{-1}) and CSH phases (800 – 1050 cm^{-1}). In point H, a hump (400-530 cm^{-1}) for amorphous silica and a peak (517 cm^{-1}) for silicon crystal were identified, indicating the existence of unreacted SF in the 22 hours' hydrated paste. As these fingerprint bands were not so clear in Fig. 5, the Raman spectrum of point H is reproduced separately in Fig. 6. Again, as the sloping background could make disturbance to the genuine bands in the Raman spectra, the background in Fig. 6 was subtracted using the same method as described in Section 3.1.2 and the resultant spectrum is shown in Fig. 7(a). As can be seen in Fig. 7(a), CSH phase (600-800 cm^{-1}), ettringite (993 cm^{-1}), carbonate (1085cm^{-1}) and carbon (1350 and 1600 cm^{-1}) have been identified. The unhydrated SF has also been clearly distinguished, as shown by the hump between 350 cm^{-1} and 550 cm^{-1}. Therefore, it can be concluded that unhydrated SF still exist in the paste after 22-hour hydration.

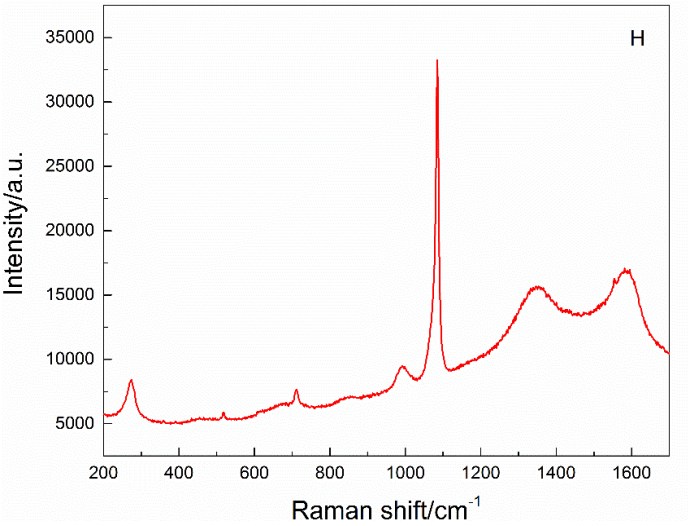

Fig. 6. Raman spectrum of the point H in Fig. 4

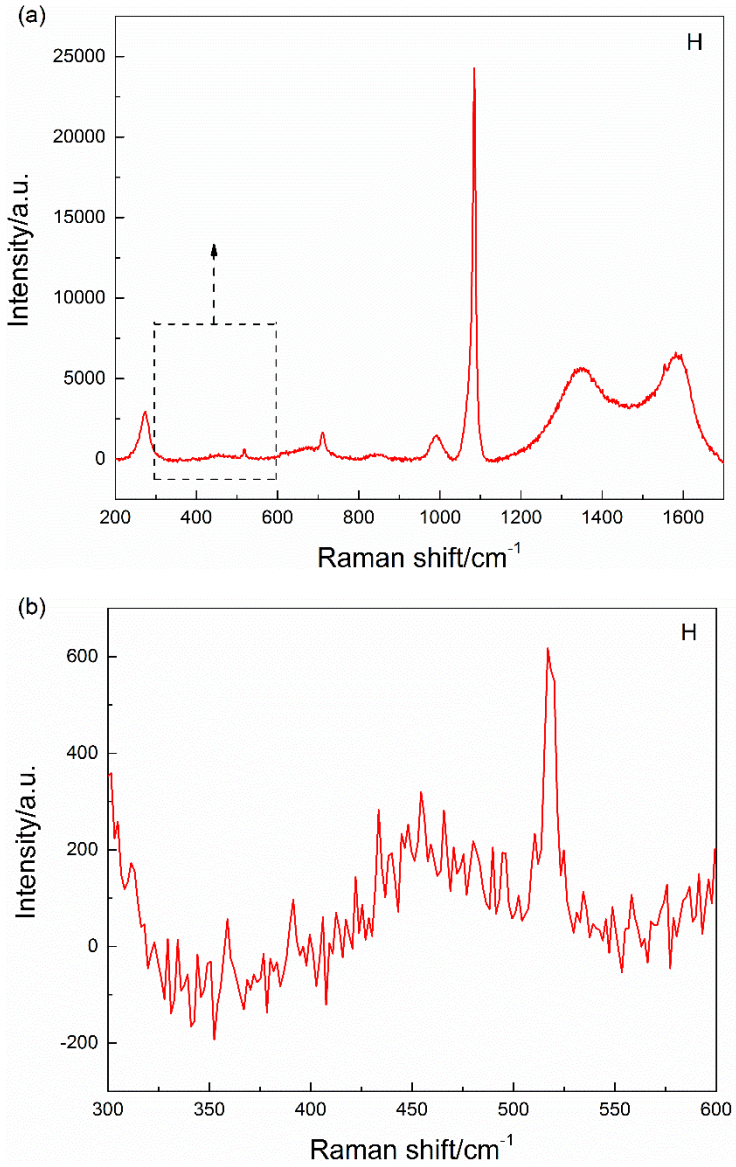

Fig. 7. (a) Raman spectrum of the point H in Fig. 4 after subtracting background. (b) Inset of Raman spectrum in the range of 300-600 cm^{-1}.

3.2.2 SF-PC blended paste after 6 months' hydration

To reveal the status of the SF in mature samples so that some useful information could be obtained to understand the possible situation of the SF in real concrete structures, the SF blended PC paste after 6-month hydration was analysed with Raman spectroscopy. Again, the light optical spectroscopy was conducted to investigate the morphology so that some typical features could be identified before carrying out the Raman analysis. As shown in Fig.8(a), an area with some typical features were selected and four analysing points, i.e. A, B, C and D, were then selected to carry out the Raman analysis.

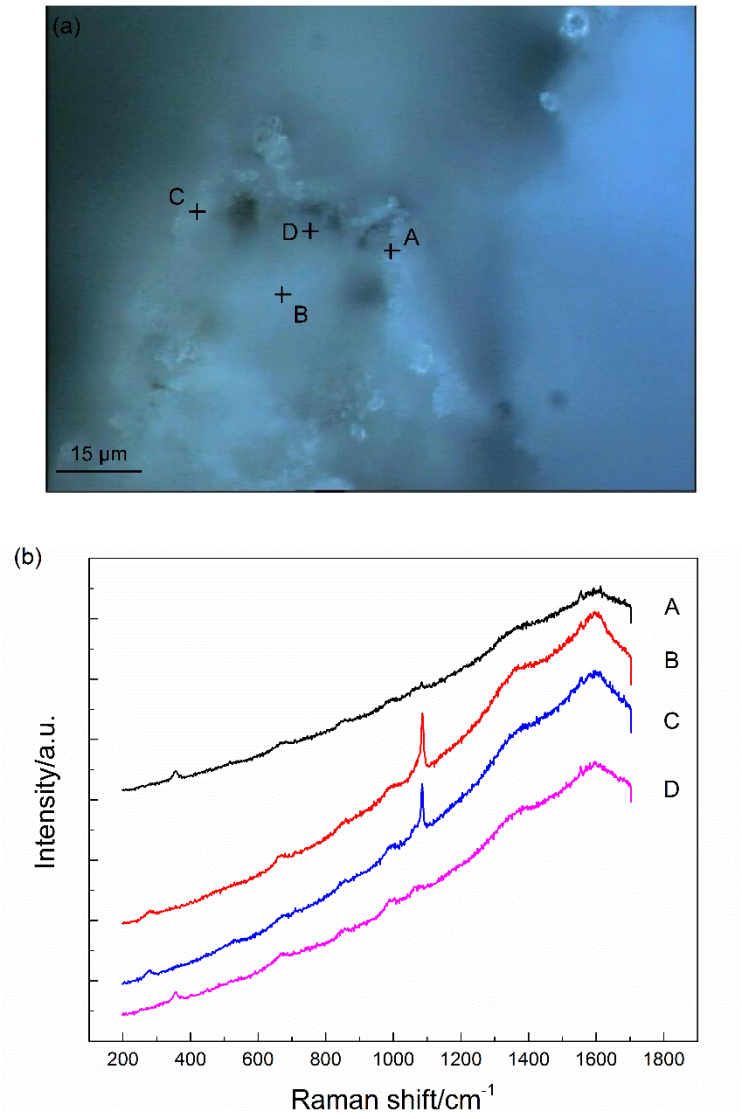

Fig. 8. (a) Light-optical micrograph of the SF-PC paste after 6-month hydration (100x). (b) Raman spectra of sampling points A-D as shown in (a).

In Fig. 8(b), the Raman spectra were accompanied by strong fluorescence, together with the broad bands near 1380 $cm^{-1}$and 1600 cm^{-1} which is the typical Raman features of carbon existed in SF[22]. On the Raman spectrum of point A, a peak located at 356 cm^{-1}wasidentified, which could be attributed to the Ca-O vibration of $Ca(OH)_2$ formed during the hydration of PC[30]. Moreover, there were three humps located at about 600-710 cm^{-1}, 820-900 cm^{-1} and 950-1020 cm^{-1}representing CSH phases viz. the first hump could be due to the Si-O-Si symmetric bending modes of CSH with different polymerisation degrees, such as Q^1, Q^2 and Q^3 whist the last two humps are the Si-O symmetric stretching of CSH such as Q^1 and Q^2[26]. At the same time, a weak peak emerged at 1084 cm^{-1}corresponds to the carbonates formed. Furthermore, unhydrated SF was also identified, as manifested by the

peaks seen at about 517 cm^{-1}. For Point B, the sharp peaks at 1085 cm^{-1} and 277 cm^{-1} could be assigned to the symmetric stretching and lattice vibration of [CO_3^{2-}] of the carbonates respectively. The humps at 620-700 cm^{-1}, 820-870 cm^{-1} and 940-1030 cm^{-1}could be associated to the vibration of CSH phases[26, 27].Moreover, the unhydrated amorphous silica was also identified by the hump around 400-530 cm^{-1} - although it is very weak, possibly due to its small quantify and the interference from the background fluorescence. Point C showed similar Raman pattern as that of Point B, within which carbonates and CSH dominated the Raman spectrum. In the case of Point D, similar Raman bands as that of Point A were obtained with CH/CSH also being identified. Additionally, a hump at 400-540 cm^{-1} was recognised, which could also be attributable to the unhydrated amorphous silica.

As previously mentioned, strong backgrounds were observed in the Raman spectra of this 6-month hydrated SF-PC paste, which could possibly interfere the genuine Raman bands. Again, to clearly identify the unhydrated SF, the background subtraction (as discussed in Section 3.1.2) was applied to Raman spectrum of point B and the resultant spectra are presented in Fig. 9 below. As shown in Fig. 9(a), after the background subtraction, the Raman bands were more evident. The sharp peak which dominated the spectrum could be attributed to the carbonates formed in the presence of atmospheric CO_2 during the sample storage. In Fig. 9(b), the hump lying at 400-530 cm^{-1}, which is the fingerprint of the amorphous silica, indicates again the existence of unhydrated SF in the 6 months' SF-PC blended paste.

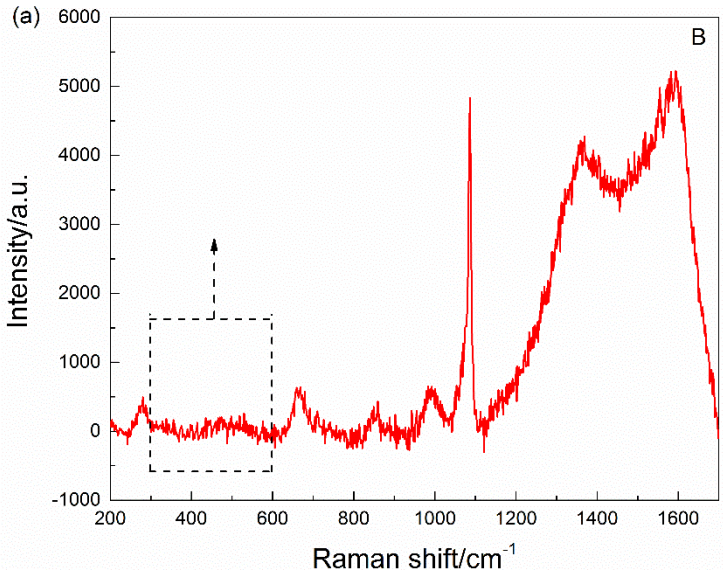

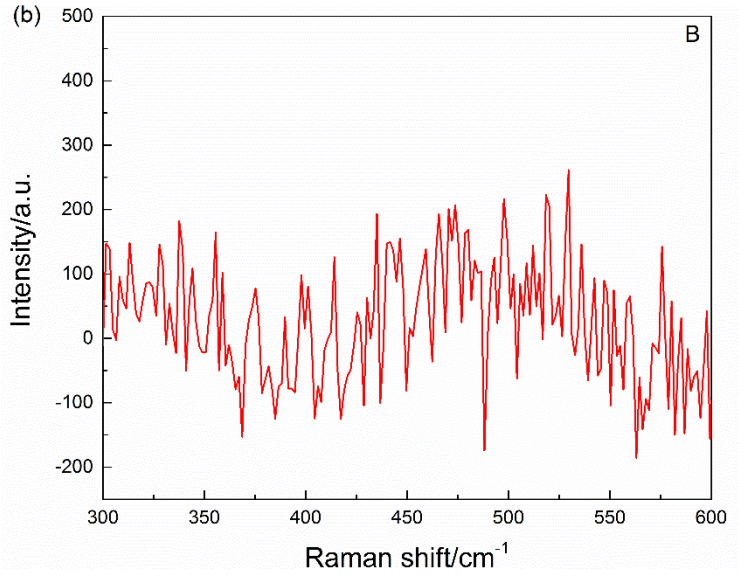

Fig. 9. (a) Raman spectrum of the point B in Fig. 8(a) after subtracting background. (b) Inset of Raman spectrum in the range of 300-600 cm^{-1}.

As discussed above, the spectra of the points A and D were very similar, as were those at points B and C.Taking into account of the optical micrograph of Fig. 8(a), the following assumption and discussion have been deduced:

(i) the area observed could be a SF agglomerate covered by layers of CH/CSH precipitates with inner core consisting of unhydrated SF particles. This is supported by the finding from the light-optical micrograph and Raman spectra which showed that the CH and CSH phases were identified at the outer area, i.e., points A and D, whilst the unhydrated amorphous $SiO_2$was identified in the inner point B. In addition, this deduction can be further confirmed by the literature which showed that the reactions between SF and CH could be retarded because of the formation of the CSH layer on the surface of SF agglomerate, which can prohibit the further reactions[12];

(ii) the SF agglomerate observed here was a partially sealed cluster, with an open channel near point C which generated some other reactions, such as the intrusion of CO_2 and then the formation of calcite as observed in points B and C.

4. CONCLUSION

This study indicates that Raman microscope which combines Raman spectroscopy with light-optical microscope offers a promising alternative for identifying both the chemical

composition and physical morphology of the SF, in particular the SF agglomerates, in cementitious materials. Specifically, under Raman analysis with an excitation laser of 488nm, various phases in original SF slurry have been successfully identified in this study, such as amorphous SiO_2 (350-540 cm^{-1}), crystalline silicon (518 cm^{-1}) and carbon (1359 and 1609 cm^{-1}). In addition, SF agglomerate in diluted SF slurry was clearly demonstrated by light-optical microscope, along with its composition being identified by Raman spectroscopy. Furthermore, SF agglomerate was also identified in both the early (22-hour) and long-term (6-month) hydrated SF-PC blended pastes. The fact that the SF agglomerates were observed in the SF-PC blend after even 6 months' hydration could raise the concern over the safety of the living systems surrounding the concrete manufactured with SF due to the small particle size of SF. In particular, during its service life, concrete is exposed to and also interact with the exposure environment (such as CO_2 and SO_4^{2-}) which could trigger further chemical reactions. Whether these unreacted SF could be released into the living system due to these deterioration reactions and, thus, cause more severe hazardous to the living systems will need further future investigations to clarify.

ACKNOWLEDGEMENT

This research was supported by the QNano Project http://www.qnano-ri.eu which is financed by the European Community Research Infrastructures under the FP7 Capacities Programme (Grant No. INFRA-2010-262163) and its partner, Centre for Research on Adaptive Nanostructures and Nanodevices (CRANN), at Trinity College Dublin. This and the cement provided by QUINN and the silica fume supplied by Elkem, are gratefully acknowledged.

REFERENCES

1. Hewlett, P., *Lea's chemistry of cement and concrete*. 2003: Butterworth-Heinemann.
2. Siddique, R., *Utilization of silica fume in concrete: Review of hardened properties.* Resources, Conservation and Recycling, 2011. **55**(11): p. 923-932.
3. Elahi, A., et al., *Mechanical and durability properties of high performance concretes containing supplementary cementitious materials.* Construction and Building Materials, 2010. **24**(3): p. 292-299.
4. Siddique, R. and M.I. Khan, *Supplementary cementing materials*. 2011: Springer Science & Business Media.

5. Isaia, G.C., A.L.G. GASTALDInI, and R. Moraes, *Physical and pozzolanic action of mineral additions on the mechanical strength of high-performance concrete.* Cement and Concrete Composites, 2003. **25**(1): p. 69-76.
6. Aïtcin, P.C., *High performance concrete*. 2011: CRC press.
7. Holsapple, M.P., et al., *Research strategies for safety evaluation of nanomaterials, part II: toxicological and safety evaluation of nanomaterials, current challenges and data needs.* Toxicological Sciences, 2005. **88**(1): p. 12-17.
8. Viswanath, B. and S. Kim, *Influence of Nanotoxicity on Human Health and Environment: The Alternative Strategies.* 2016.
9. Hoet, P.H., I. Brüske-Hohlfeld, and O.V. Salata, *Nanoparticles–known and unknown health risks.* Journal of Nanobiotechnology, 2004. **2**(1): p. 12.
10. Diamond, S., S. Sahu, and N. Thaulow, *Reaction products of densified silica fume agglomerates in concrete.* Cement and Concrete Research, 2004. **34**(9): p. 1625-1632.
11. Diamond, S. and S. Sahu, *Densified silica fume: particle sizes and dispersion in concrete.* Materials and Structures, 2006. **39**(9): p. 849-859.
12. Mitchell, D., I. Hinczak, and R. Day, *Interaction of silica fume with calcium hydroxide solutions and hydrated cement pastes.* Cement and Concrete Research, 1998. **28**(11): p. 1571-1584.
13. Long, D.A., *Raman spectroscopy.* New York, 1977: p. 1-12.
14. Larkin, P., *Infrared and Raman spectroscopy: principles and spectral interpretation*. 2011: Elsevier.
15. BSI, BS EN 197-1:2011.*Cement Part 1: Composition, specifications and conformity criteria for common cements*. 2011.
16. Buscarino, G., et al., *Sintering process of amorphous SiO_2 nanoparticles investigated by AFM, IR and Raman techniques.* Journal of Non-Crystalline Solids, 2011. **357**(8): p. 1866-1870.
17. Bogomolov, V., et al., *Three-dimensional array of silicon nanoscale elements in artificial SiO_2 opal host.* Journal of Non-Crystalline Solids, 2000. **266**: p. 1021-1024.
18. Iqbal, Z., et al., *Raman scattering from small particle size polycrystalline silicon.* Solid State Communications, 1981. **37**(12): p. 993-996.
19. Shabir, Q., et al., *Medically biodegradable hydrogenated amorphous silicon microspheres.* Silicon, 2011. **3**(4): p. 173-176.
20. Kingma, K.J. and R.J. Hemley, *Raman spectroscopic study of microcrystalline silica.* American Mineralogist, 1994. **79**(3-4): p. 269-273.
21. Rodgers, K. and W. Hampton, *Laser Raman identification of silica phases comprising microtextural components of sinters.* Mineralogical Magazine, 2003. **67**(1): p. 1-13.

22. Ferrari, A. and J. Robertson, *Resonant Raman spectroscopy of disordered, amorphous, and diamondlike carbon.* Physical Review B, 2001. **64**(7): p. 075414.
23. Lakowicz, J.R., *Introduction to fluorescence*, in *Principles of fluorescence spectroscopy*. 1999, Springer. p. 1-23.
24. Gabrielli, C., et al., *In situ Raman spectroscopy applied to electrochemical scaling. Determination of the structure of vaterite.* Journal of Raman Spectroscopy, 2000. **31**(6): p. 497-501.
25. Wehrmeister, U., et al., *Raman spectroscopy of synthetic, geological and biological vaterite: a Raman spectroscopic study.* Journal of Raman Spectroscopy, 2010. **41**(2): p. 193-201.
26. Garbev, K., et al., *Structural features of C–S–H (I) and its carbonation in air—a Raman spectroscopic study. Part I: fresh phases.* Journal of the American Ceramic Society, 2007. **90**(3): p. 900-907.
27. Kirkpatrick, R.J., et al., *Raman spectroscopy of CSH, tobermorite, and jennite.* Advanced Cement Based Materials, 1997. **5**(3): p. 93-99.
28. Ibáñez, J., et al., *Hydration and carbonation of monoclinic C_2S and C_3S studied by Raman spectroscopy.* Journal of Raman Spectroscopy, 2007. **38**(1): p. 61-67.
29. Martinez-Ramirez, S., M. Frías, and C. Domingo, *Micro-Raman spectroscopy in white portland cement hydration: long-term study at room temperature.* Journal of Raman Spectroscopy, 2006. **37**(5): p. 555-561.
30. Tarrida, M., et al., *An in-situ Raman spectroscopy study of the hydration of tricalcium silicate.* Advanced Cement Based Materials, 1995. **2**(1): p. 15-20.